MATEC Web of Conferences **165**, 21005 (2018) https://doi.org/10.1051/matecconf/201816521005
FATIGUE 2018

A numerical analysis of multiaxial fatigue in a butt weld specimen considering residual stresses

Iñigo Llavori[1*], *Unai* Etxebarria[1], *Arkaitz* López-Jauregi[1], *Ibai* Ulacia[1], *Done* Ugarte[1], *Jon Ander* Esnaola[1], and *Miren* Larrañaga[1*]

[1]Escuela Politécnica Superior – Mondragon Unibertsitatea, Loramendi 4, 20500 Arrasate-Mondragon (Gipuzkoa). Spain.

Abstract. Residual Stress (RS) pattern changes considerably depending on the width of the plates and the welding parameters, having effect on the fatigue strength. Most of the standards do not consider them and in some works, yield stress is taken as residual stress value. It results in a very conservative estimation of fatigue life. Authors developed recently a numerical model to predict more properly the value of RS pattern depending on the plate thickness. In a welded joint, considering the RS and alternating axial loads, the evolution of the stresses is multiaxial, becoming necessary its study. Therefore, the aim of this work is to analyse different fatigue indicator parameters (Smith-Watson-Topper, Fatemi-Socie, and Critical Plane implementation of the Basquin equation) in order to predict the fatigue behaviour of butt-weld components. For that purpose, the numerical model to predict the RS pattern in welded joint developed by this research group is used.

1 Introduction

Welding process is one of the most used joining methods in the metal manufacturing industry [1]. Gas metal arc welding (GMAW) is widely used, due to its high productivity. Specially, spray transfer mode multipass welding is suitable in the case of high thickness structures [2, 3] because of the high rate of metal transfer, good arc stability, absence of weld spatter and uniform and regular metal transfer to the workpiece.

However, in welding joints, there are different variables that have a negative effect on the fatigue life [4], such as residual stresses, the inhomogeneous geometry of the welding cord or the generation of areas with different mechanical properties. Therefore, the main failure mode of welded joints is the fatigue fracture [5, 6].

Residual stresses (RS) are generated due to the high thermal gradients of the welding process, where there are non-uniform heating and cooling cycles [4]. The thermal expansion of the material is constrained by the adjacent areas that are not at the same temperature; in addition, these areas at higher temperature have lower strength, and consequently, can suffer compressive plastic deformation. During the cooling down process, the yielded areas limit the elastic springback of not yielded areas, generating internal stresses that remain on the welded component. These RS can be tensile or compressive, depending on the limitations imposed by the surrounding areas. The final RS pattern relies on different factors, such as, mechanical restraints, welding sequence, preparation of the weld groove, the number of weld passes or structure dimensions [7, 8].

On the one hand, the estimation of RS pattern due to welding process is complex due to the multi-physics phenomena as heat, electricity or mechanical work that take part in the process. On the other hand, the experimental measurement of RS nowadays presents some limitations as the methods available are not fully reliable and imply huge time and economic cost [8, 9]. Therefore, most of the fatigue life prediction approaches do not take into account RS or consider the yield stress value as RS magnitude [10, 11, 1]. This results in very conservative life estimation, and thus, in oversized designs.

In recent works, authors have presented a numerical methodology for RS pattern estimation in spray transfer multipass welding [12, 13]. This methodology enables an accurate estimation of the RS generated, based on the heat source and the welding speed. This is the methodology employed in this work to consider the RS of a butt-welded joint.

Because of the presence of the RS, when we apply a remote uniaxial load to a welded component, a multiaxial evolution of the loading-unloading cycle is generated. In other words, there is a multiaxial stress state independently of the applied load.

In this work, we have used different multiaxial parameters to estimate the fatigue life of a butt-welded component under uniaxial loading conditions, considering the RS. The objective is to evaluate and to analyse the suitability of each multiaxial parameter for the studied case.

* Corresponding author: mlarranaga@modragon.edu , illavori@mondragon.edu

2 Numerical methodology for residual stress estimation

In order to solve the thermal and mechanical fields along the welding process, we have used an uncoupled thermos-mechanical model implemented in the simulation software ABAQUS FEA (Fig. 1). This approach is accepted as dimensional changes in the welding process can be neglected and mechanical deformation energy is insignificant compared to the thermal energy from the welding arc [14]. Both equation systems, thermal and mechanical, are solved by using the implicit direct integration method.

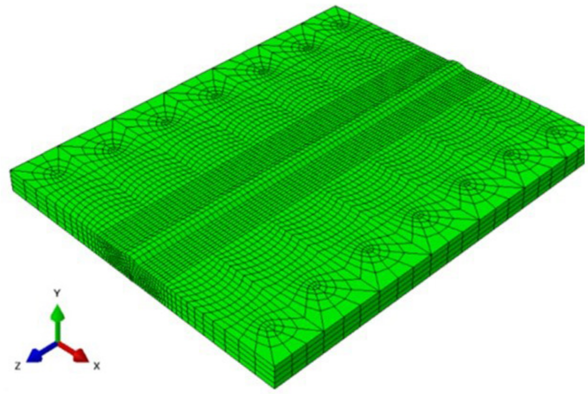

Fig. 1. Modelling of the simulation process [12]

For both models (thermal and mechanical) full integration continuum hexahedral elements and the addition of filler material through all passes is modelled by using the kill/rebirth method [2, 3]. In this method, all the weld bead elements are initially inactive and, consequently, eliminated (killed) from the equation system. Then, according to the welding speed and material addition discretization size, elements are reactivated (rebirthed) simulating the welding torch pass (Fig. 2) [15].

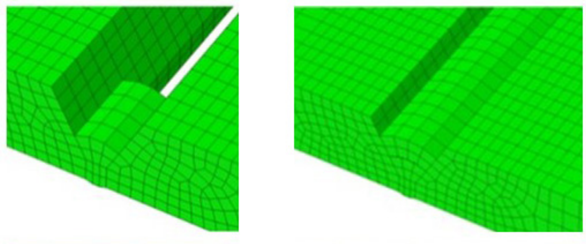

Fig. 2. Simulation of the welding process

The main input parameters needed for the numerical simulation are the welding speed and the heat source power. These parameters have been defined according to the analytical procedure proposed by the authors in [12].

The results obtained by this numerical method were compared to experimental results, obtaining a very good agreement. Therefore, we can say that this numerical prediction method is widely validated [12, 13, 16, 17].

3 Multiaxial fatigue

Material fatigue refers to a progressive degradation of a material caused by loading and unloading cycles. The stress fluctuations suffered over time weakens or breaks the material even at stresses lower than the yielding value. Accordingly, lot of effort has been directed at developing fatigue life prediction models. Fatigue is characterized with a high scatter of the lifetime. Probabilistic approaches are recently arising in the literature to address this problem. However, the majority of the models currently used analyses fatigue in a deterministic way, *i.e.* a structure fails if a given parameter reaches a critical value.

Nowadays, a variety of different approaches for fatigue life prediction exists, such as approaches based on multiaxial fatigue criteria, damage mechanics or micromechanics, which are extensively reviewed in literature. Multiaxial fatigue criteria reduces the multiaxial stresses (usually computed by FEM analysis) to an equivalent uniaxial stress state. This way, the results can be compared to an experimental fitting curve obtained from uniaxial fatigue data. A crucial step when selecting a multiaxial criterion is to check whether the simplification from multiaxial stress state to an equivalent uniaxial stress state are acceptable or valid. This task is not simple and requires the detailed study of the evolution of stresses and strains along the loading cycle.

The book published by Socie and Marquis [18] presents a wide and detailed study about the principal multiaxial parameters, also known as Fatigue Indicator Parameters (FIPs). Those parameters can be broadly classified into three groups: strain-based, stress-based and energy-based FIPs. Strain-based FIPs are generally related with Low-Cycle Fatigue (LCF) where plastic deformation may be predominant. Stress-based FIPs are associated with High-Cycle Fatigue (HCF) where the stresses usually remains in the elastic domain. Finally, energy-based models relates the product of stresses and strains to quantify fatigue life, which generally are applicable to both LCF and HCF regime.

For these complex stresses or loading states, other approaches such as the critical plane method are more suitable. The critical plane method has been developed from the experimental observation of nucleation and crack growth under multiaxial loading. The critical plane models include the dominant parameters that govern the type of crack initiation and propagation. An adequate model must be one that estimates correctly both fatigue life and the dominant failure plane. However, several failure modes exists, and there is not a unique parameter that suits all. Nonetheless, the most popular parameters are the energetic criteria known as Fatemi-Socie (*FS*) [19] and Smith-Watson-Topper (*SWT*) [20].

The *SWT* parameter is applied in those materials where the crack growth occurs in mode I. The critical plane is defined as the one where the product of maximum normal stress ($\sigma_{n,max}$) and normal strain amplitude ($\varepsilon_{n,a}$) is maximum.

$$SWT = \left(\sigma_{\mathrm{n,máx}}\varepsilon_{\mathrm{n,a}}\right)_{\mathrm{máx}} = \frac{\sigma_{\mathrm{f}}^{'2}}{E}\left(2N_{\mathrm{f}}\right)^{2b} \qquad (1)$$

where $\sigma_{\mathrm{f}}^{'}$ is the fatigue strength coefficient, b is the fatigue exponent, and N_{f} is the number of cycles to failure.

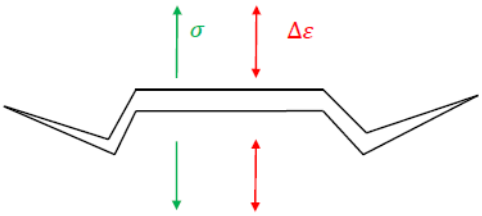

Fig 2. Physical base of the *SWT* parameter.

Under shear loading condition, crack lip surfaces generate frictional forces that reduce stresses at the crack tip, thus increasing fatigue life. However, tensile stresses and strains will separate the crack surfaces, reducing the friction forces. The energetic FIP *FS* can be understood as the cyclic shear strain to include the crack closure effect multiplied by normal stress to take into account the opening of the crack.

$$FS = \frac{\Delta\gamma_{\max}}{2}\left(1 + k_{\mathrm{FS}}\frac{\sigma_{\mathrm{n,max}}}{\sigma_{\mathrm{y}}}\right) = \left(1+\nu\right)\frac{\sigma_{\mathrm{f}}^{'}}{E}\left(2N_{\mathrm{f}}\right)^{b} + \frac{k_{\mathrm{FS}}}{2}\left(1+\nu\right)\frac{\sigma_{\mathrm{f}}^{'2}}{E\sigma_{\mathrm{y}}}\left(2N_{\mathrm{f}}\right)^{2b} \qquad (2)$$

where $\Delta\gamma_{\max}$ is the maximum range of shear strain on any plane, $\sigma_{\mathrm{n,max}}$ is the maximum normal stress in that particular plane, σ_{y} is the material yield stress, k_{FS} is a material dependent factor.

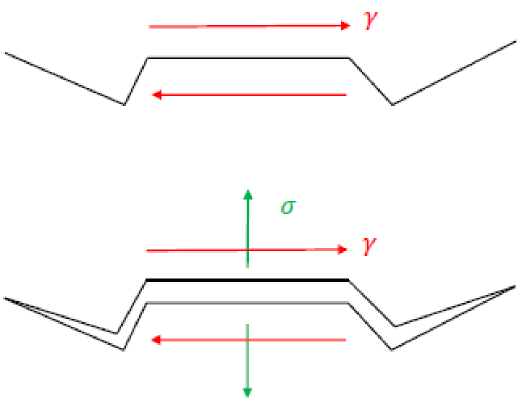

Fig 3. Physical base of the FS parameter.

The last parameter used in this work is the procedure used previously by the authors. In this case, it was assumed that the fatigue life estimation of welded structures can be conducted considering only the crack propagation [1]. For this reason, maximum normal stress criterion [21] based on Papadopoulos *et al.* [22] where influence of the shear stress is neglected, was used. This method is based on the critical plane implementation of the Basquin equation. The linear interaction between the stress amplitude and mean stress defined by Goodman were used to take into account the influence of RS on the fatigue strength.

$$\frac{\sigma_{\mathrm{a\text{-}res}}}{\sigma_{\mathrm{e}}} + \frac{\left(\sigma_{\mathrm{mean}} + \sigma_{\mathrm{res}}\right)}{\sigma_{\mathrm{u}}} = 1 \qquad (3)$$

where σ_{e} is the endurance limit at 10^7 cycle for the base material, and σ_{u} is the ultimate tensile stress (525 MPa for the studied case), $\sigma_{\mathrm{a\text{-}res}}$ is the stress amplitude considering RS, σ_{mean} is the mean stress and σ_{res} is the numerically estimated welding RS value in the critical plane of the studied zone. For fully reversed case (R = -1), the previously defined equation is written as follows.

$$\frac{\sigma_{\mathrm{a\text{-}res}}}{\sigma_{\mathrm{e}}} + \frac{\sigma_{\mathrm{res}}}{\sigma_{\mathrm{u}}} = 1 \qquad (4)$$

4 Case study

The component analysed in this work is formed by two butt-welded S275JR 10 mm-thick plates. Filler material 1.2 mm diameter PRAXAIR M-86 filler wire, according to the AWS/ASNE SFA 5.18 ER70S-6 standard, and quasi-constant weld pass section were considered.

We have obtained the numerical estimation of the RS pattern by the methodology described in section 2 (Fig. 3).

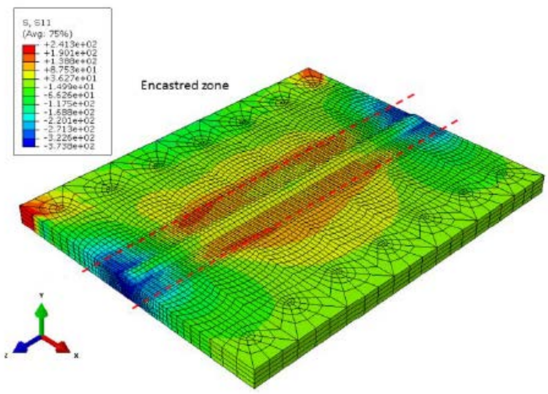

Fig. 3. Residual stress pattern numerically estimated [12].

We have analysed the RS stress pattern along the whole welding cord. As can be observed in Fig. 3, the maximum stresses appear at the middle of the cord. We have chosen the most stressed element in order to do this analysis.

After obtaining the RS pattern due to welding process, we applied a uniaxial remote load perpendicular to the welding cord. We recorded the evolution of stresses and strains of a complete loading-unloading cycle for the most stressed element in the welding cord.

5 Results

The experimental results for numerical correlation have been taken from previous work done by the authors [13], and they are summarized in Table 1. Additionally, HCF calibrated parameters for the base material S275JR is summarized in Table 2.

Table 1. Experimental results of butt-weld specimens at R = -1, performed by force control in a conventional fatigue machine MTS 810.

Test	σ_a [MPa]	N_f [cycles]
1	125	133880
2	125	139649
3	125	233312
4	125	292178
5	125	965456
6	115	355750
7	115	371078
8	110	538638
9	110	1159103
10	110	1243530
11	110	1352999
12	110	1461791
13	110	1579331
14	90	1080407
15	90	1431281
16	90	1977803
17	90	2244631
18	80	9895092

Table 2. Calibrated Basquin parameters for S275JR base material.

σ_f' [MPa]	b [-]
415.48	-0.047

Fig. 3 shows the prediction of the employed FIPs comparing with experimental results. As previously commented, the fatigue life estimation results are based on the stresses and strains of a specific element at the middle of the welding cord.

On the one hand, it can be observed that the *SWT* parameter shows the best correlation because it takes into account the effect of mean stress (through the maximum stress) and strain amplitude.

On the other hand, the worst correlation is the one presented by the *FS* parameter. This may be because in these tests, the applied load is uniaxial and the effect of the residual stresses on the shear stress is negligible. Finally, the prediction of critical plane implementation of the Basquin model is the most conservative due to the use of the Goodman equation that is described in the literature as a conservative [23].

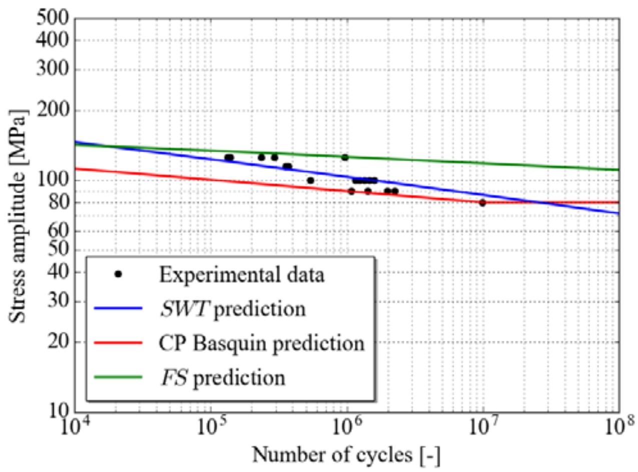

Fig. 4. Fatigue Indicator Parameters prediction vs.experimental tests.

Fig. 4, Fig. 5 and Fig. 6 show the correlation between the predicted stress amplitude (σ_{predic}) and the experimental ones (σ_{exp}) for the 3 parameters analysed. The mean absolute percentage error (*MAPE*) has been calculated as:

$$MAPE = \frac{100}{m}\sum_{j=1}^{m}\frac{\left|\sigma_{exp,j} - \sigma_{predic,j}\right|}{\sigma_{exp,j}} \quad (5)$$

The computed error therefore for each parameter is:

- *SWT* = 6.19%
- *FS* = 24.21%
- *CP* Basquin = 10.45%.

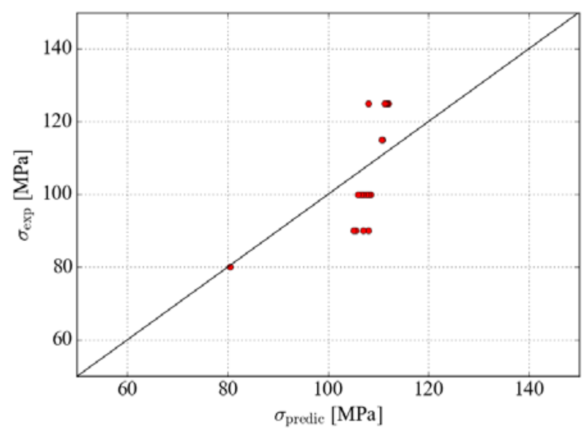

Fig. 5. Experimental stress amplitude, σ_{exp}, vs predicted stress amplitude, σ_{predic}, by *CP* Basquin parameter.

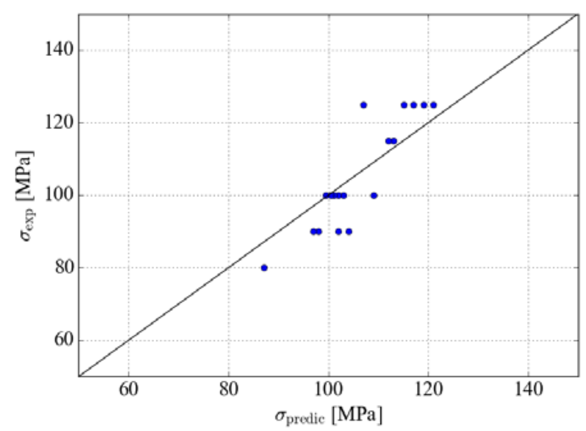

Fig. 6. Experimental stress amplitude, σ_{exp}, vs predicted stress amplitude, σ_{predic}, by *SWT* parameter.

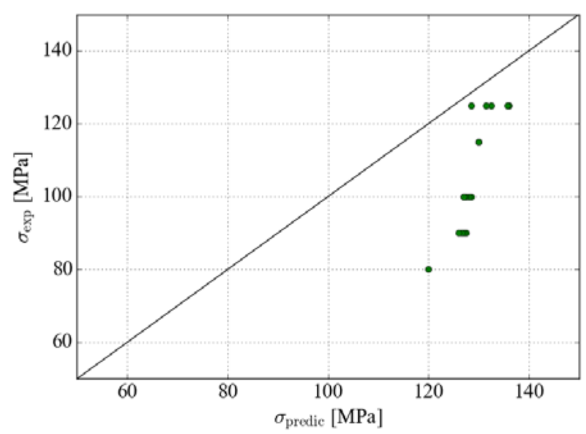

Fig. 7. Experimental stress amplitude, σ_{exp}, vs predicted stress amplitude, σ_{predic}, by *FS* parameter.

These results suggest that the *SWT* parameter can be a good indicator to predict the fatigue lifetime of butt-weld specimens.

However, the results obtained are based on the stress and strain state of only one element. In order to obtain more representative results, the next step of this research will be to evaluate the FIPs at all the elements of the welding cord.

In addition, we have analysed one loading case (uniaxial loading). As we have observed in the results, each FIP may be more suitable for a different loading condition. Thus, a wider analysis is recommended, taking into account different loading cases.

6 Conclusions

In this study different fatigue indicator parameters (*SWT*, *FS*, and *CP* Basquin) have been used in order to predict the fatigue life of butt-weld specimens. This study has been analysed with a numerical procedure proposed by the authors in order to predict the effect of RS on fatigue life.

The numerical results suggest that the *SWT* parameter is a suited FIP to predict the fatigue life of butt-weld specimens.

References

1. T. Lassen, N. Recho, *Fatigue life analyses of welded structures*. Iste London (2006).
2. M. Mousavi, M. Haeri, ISA T **50** (3), 409-418 (2011).
3. P. E. Murray, Weld. J. **81** (7), 125-131 (2002).
4. S. J. Maddox, *Fatigue strength of welded structures*, Woodhead publishing (1991).
5. A. Carpinteri, A. Spagnoli, S. Vantadori, Int J Fatigue **31**, 188-196 (2009).
6. P. Livieri, P. Lazzarin, Int. J. Fracture **133** (3): 247-276 (2005).
7. B. Brickstad, B. L. Josefson, Int. J. Pres. Ves. Pip. **75** (1):11-25 (1998).
8. M. Asadi, J. Goldak, J. Nielsen, J. Zhou, S. Tchernov, D. Downey, Int. J. Mech. Mater. Des. **5**, 353-364 (2009).
9. A. Paradowska, J. W. Price, R. Ibrahim, T. Finlayson, J. Mater. Process. Technol. **164**, 1099-1105 (2005).
10. C. M. Sonsino, Int. J. Fat. **31** (1), 173-187 (2009).
11. D. Radaj, C. M. Sonsino, W. Fricke, *Fatigue assessment of welded joints by local approaches*, Woodhead publishing (2006).
12. A. Lopez-Jauregi, I. Ulacia, J.A. Esnaola, D. Ugarte, I. Torca, J. Larrañaga, Int. J. Adv. Man. Tech. **76**, pp. 2117-2129 (2014).
13. A. Lopez-Jauregi, J. A. Esnaola, I. Ulacia, I. Urrutibeaskoa, A. Madariaga, Int. J. Fat. **79**, pp. 75-85 (2015).
14. Safety data sheet for Stargon 82, http:/www.cialgas.com/wpcontent/uploads/2012/09/STARGON-82.pdf. Accessed 11 June 2014.
15. J.A.Esnaola, I. Ulacia, A. Lopez-Jauregi, D. Ugarte. Residual Stress Pattern Prediction in Spray Transfer Multipass Welding by Means of Numerical Simulation. Book chapter. ISBN 978-953-51-5765-6. Accepted.

16. J. A. Esnaola, I. Ulacia, D. Ugarte, A. Lopez-Jauregi, I. Torca, J. Larrañaga, *Proceedings of the ASME IMECE* (2016).
17. J.A. Esnaola, A. Lopez, I. Ulacia, D. Ugarte, I. Torca, J. Larrañaga, *Materials today*, Interjoin (2016).
18. D. Socie, G. Marquis, *Multiaxial Fatigue*, SAE (2000).
19. A. Fatemi, D.F. Socie, Fatigue Fract Eng M. 187(1): 149-165 (1988).
20. R.N. Smith, P. Watson, T.H. Topper. J. Mater. **5**, No. 4, pp. 767-778 (1970).
21. A. Karolczuk, E. Macha, Int. J. Fract. **134**, 267-304 (2005).
22. I. Papadopoulos, Fatigue Fract. Eng. Mater. Struct. **21**, 269-85 (1998).
23. N. Meyer, Phd Thesis, University of Toledo, USA (2015).